3D design and study of field quality of an opposite field septum magnet

Summary report of the summer studentship programme "2020-1.2.1-GYAK" of the National Research, Development and Innovation Office, Hungary

Marcell Szakály (supervisor: Daniel Barna)

July-September 2020

Contents

1 Introduction

An iron-free superconducting opposite field septum magnet was proposed in [1] as a compact solution to generate a large jump in magnetic field over a small distance, for the extraction of charged particle beams from accelerator rings. A possible application of this magnet is in the planned compact superconducting medical accelerator, to be developed in the framework of the EU proposal "HITRIplus". Since an opposite-field septum magnet creates a magnetic field in both of its apertures, the magnet would be an active part of the ring optics. Therefore the same stringent field quality requirements apply for the magnet, as for the ring elements. Although the 2D field quality was shown[1] to be sufficient, the 3D coil geometry, including the coil ends, can degrade this quality, besides being non-trivial to design and construct. This report summarizes possible 3D coil designs, and presents the field quality studies of these configurations.

2 Design

The cross section of the magnet coil is shown in Figure 1. The magnet would be constructed dominantly from three parts, which are illustrated schematically in Fig. 2: two long aluminium formers, one for each

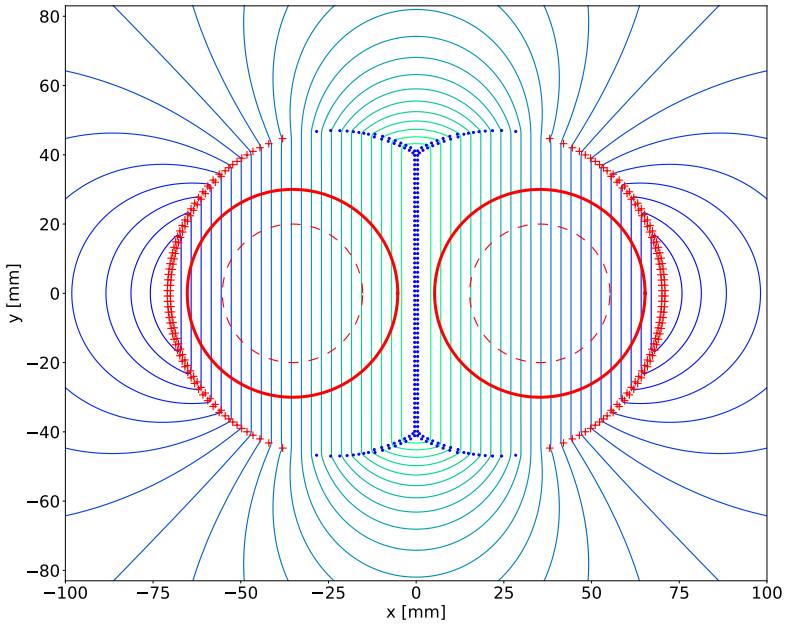

Figure 1: A cross section of the opposite field septum. Red pluses and blue dots are the positive and negative currents respectively. The large red circles are the aperture of the magnet, the dashed red circles indicate the good-field region, at 2/3 of the aperture.

aperture, and a larger "support tube" into which the two formers can be slid in longitudinally. For the 3D coil ends extra spacers (not shown in Fig. 2) are planned, which can be machined by 5-axis CNC machines, or 3D printed.

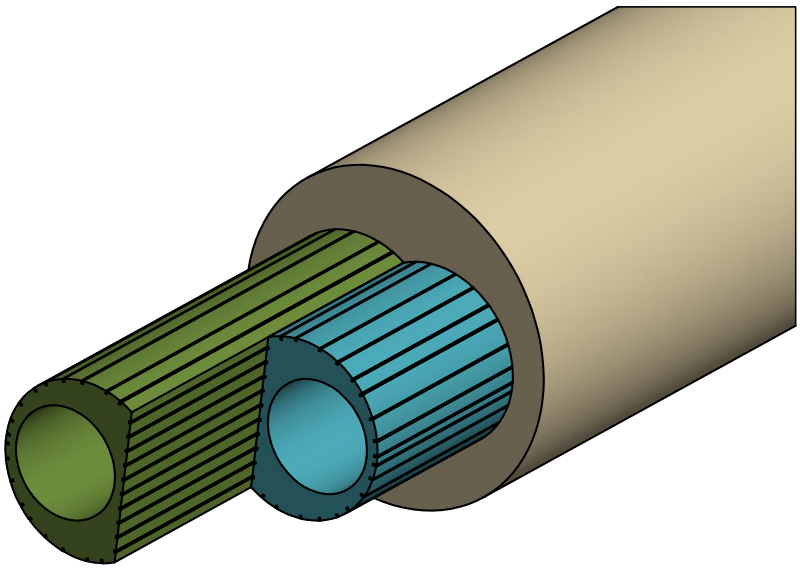

Figure 2: Schematic illustration of the construction principle. The spacing of the longitudinal grooves is not realistic. The end spacers for the coil ends are not shown.

The cables will be placed in long slots cut into the outer side of the formers. The main challenge when

designing this magnet is to find a place for the wires to turn back at the ends, leaving the two apertures unobstructed. Since both halves of the magnet will be constructed from a single long superconducting strand, it is important to design the cable path in a way that is possible (or ideally: easy) to wind.

Due to the spring-back of the NbTi wire with a diameter of approximately 0.85 mm at the small curvatures of the coil ends, the wire will be prone to popping out from the guiding channels. The wires therefore need to be individually supported during the winding process.

The wire routing algorithm used in this work is based on the following concepts, nomenclature and coordinate system. The z axis points along the magnet (i.e. perpendicular to the plane of Fig. 1), and is located at the magnet's center. The x axis points across the two apertures. The axial grooves along the length of the formers (also shown in Fig. 2), and the associated straight segments of the wire path are called *slots*. A wire exiting from a slot has first a short segment with a 3D trajectory. The radius of curvature of these segments is chosen to be about 10 times the wire diameter, i.e. 8 mm. The wire then passes to the target slot (with opposite current polarity) in a z=const plane. These segments are grouped into (and snapped to) *layers* at specific (and regularly spaced) z coordinates. The wire trajectories within a layer are organized into groups with overlapping projections to the transverse plane for most of their length. These projections are equally spaced concentric arcs around the aperture's centre, and are called *tracks*.

The algorithm described below was implemented in python. It takes as input the 2D coordinates of the wire positions, and outputs the 3D path of the complete winding.

Thanks to this quantization and separation of the problem, we can split it into three distinct parts:

2.1 The Plan

The plan outlines the general route we want the wire to follow. It lists the order in which the wire will pass through the slots, tracks and layers. All that's left is to connect these key points with nice curved segments. Our goal was to wind an aperture with a single wire, without a soldered joint.

This is by far the most complicated step, as it is important to make a plan that is easy to execute, both for the subsequent stages, and during the winding process. There are two simple fundamental ways to tackle this problem.

Track first: In the track first approach, our goal is to first fill up all layers in a given track, and then proceed to the next track. In this approach, the entire end of the magnet can be constructed from a single block of material, with deep grooves for each track, and some additional grooves, for the part where the various layers in a track split to their respective slots. This is quite hard to machine, since the tracks are all very deep ($\approx$1.5 cm) and narrow ($\approx$1 mm) channels, however this is not the only difficulty. Since the wires in a track are directly on top of each other, the effective layer separation is only as much as the wire diameter. This means that the wires have to spread out sideways before beginning to descend into their slots. Due to the limited space, this is not possible. We were not able to find any simple (eg. solderless) solution in this approach.

Layer first: In layer first winding, our goal is to fill each track in the first layer, before proceeding to the next layer. In this approach, the end spacer of the magnet would consist of several individual parts, one for each layer, with the tracks machined into these parts as grooves. When a layer was wound, a new spacer sheet can be added, thus fixing the wires of the previous layer. This has the added benefit of allowing us to increase the layer separation, practically arbitrarily. While in general, we would want to keep the width of the magnet ends at a minimum in order to improve the field quality, a larger layer separation makes the realization of the coil end configuration much easier.

Since each track is associated with a different section of the magnet (neighbouring set of slots), filling all tracks in a given layer will mean that the wire initially goes from the top of the magnet (in the y direction) to the bottom with large jumps across the slots. Then it goes to the next layer, and goes from bottom to top in a similar fashion. Only after many layers of zigzagging through the magnet does the wire finally reach all slots.

In our case, the magnet had 108 positive and 108 negative wires per aperture. Preliminary calculations from the available track number due to the aperture showed that slightly above 10 layers would be needed, so a number of 12 was chosen, as it is a divisor of 108. This meant that we could exploit some periodicity in the problem when using this zigzagging approach.

2.2 Construction of track projections

In this step we only construct the projections of the tracks and their connecting segments to the transverse plane. The plan gives a big list of wire segments that need to go from one slot, through a given track, to another slot. The connecting pieces between tracks and slots are determined as arcs with end points at the slot's projection and on the track. These arcs are constrained to be tangential to the track, with radius of about the radius of curvature defined before, with constraints to handle edge cases.

2.3 3D paths

Finally the 2D projections are "extruded" to 3D using the following algorithm. Let s mean the path length along the projected connecting segment, starting at the slot. The segment's z coordinate is defined as $z = \sqrt{R^2 - (R - s)^2}$ (i.e. "circle-like"), where R is the bending radius defined above. In addition, the track and the connecting segments are snapped to the z coordinate of their layer. In this step we also create a co-moving reference coordinate system of the track and the connecting segment. Since grooves will be cut using a CNC machine, we do this in a way so that one of the axes points in the direction the CNC will cut from. For the central part of the track, this is trivially the z axis. At the slots, this is normal to the surface of the formers. In the small connecting region between these, interpolation is used.

2.4 Full cable path

For use in the simulation step, we need to output the entire wire geometry. This is done by outputting the coordinates and the co-moving system every 0.2 mm along the wire path. So far, the co-moving system was only defined for each end segment. Since at the ends of these segments, the co-moving frame is always aligned with the surface normal of the former, the co-moving system in each straight slot can be trivially defined.

3 Evaluation

3.1 Simulation

Simulations were done using RAT [2], a software which uses the MLFMM method to solve magneto static problems in free space very fast, compared to other industry standard FEM software. The wire was exported as a long list of coordinates, and a local coordinate system, tangential and a normal vector. The third vector (another normal direction) was calculated as a cross product of the two. The two halves of the magnet are assumed to be the same, down to rotation/mirror freedom. In total we have 4 possible relative orientations. These will have slightly different field qualities, however it was found that the difference is completely negligible. Hence we choose the simplest configuration to construct, which is where the two sides of the magnet are mirror images of each other, across the $y - z$ plane. This is because in this configuration the wire endings of the magnet are close together, so can be connected with minimal effort.

The field quality was calculated at the radius indicated in Figure 1, at 2/3 of the aperture. The field was sampled at 120 equally spaced angles around the axis of the aperture, every 1 mm for a length of 2 m along the z axis, over twice the length of any of the magnets tested.

3.2 Field quality

The field quality was calculated for magnets of various length, and with different end layer separation. The total physical length is defined to include the end, as it would in a real magnet.

Figure 4 show the magnitudes of the dipole and quadrupole normal field component as a function of the longitudinal coordinate, for magnets with different lengths, and a layer spacing of 3.6 mm (the smallest realizable spacing without intersecting wire paths). This gives a total thickness of the coil end of about 40 mm.

Since the 2D coil geometry was shown to produce a very high-quality field[1], the contribution to the higher-order multipoles are associated with the 3D coil ends. Therefore we expect each integrated multipole component to be a linear function of the length, with an offset. This offset is from the end of the coils,

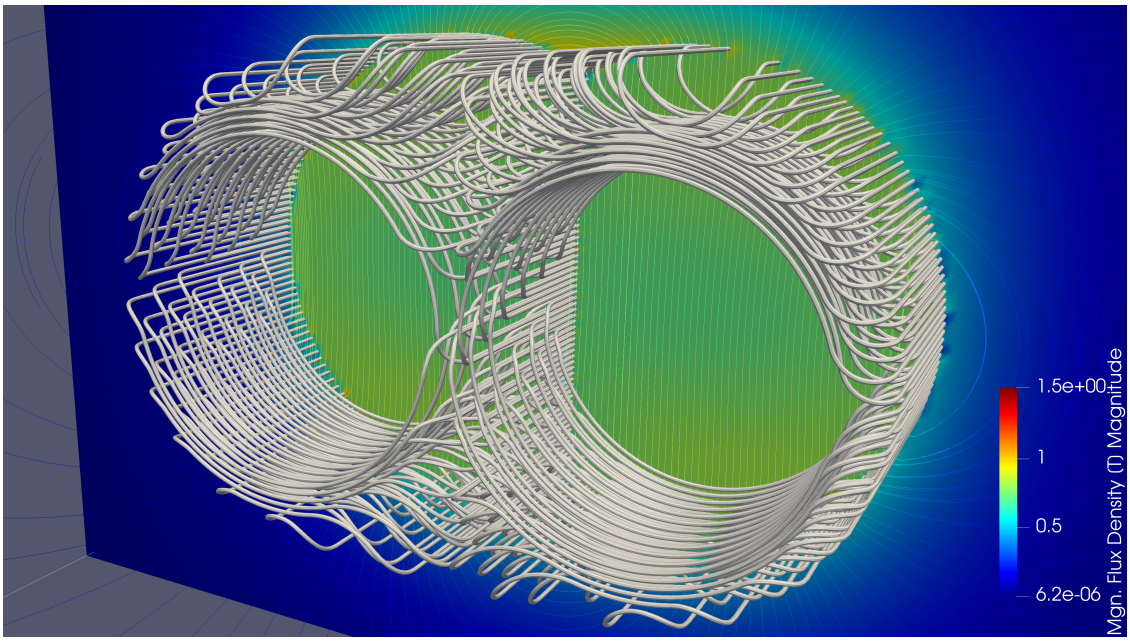

Figure 3: A visualisation of the end of the magnet, with the induction lines in the transverse plane.

while the linear component is from the slight imperfection due to the discrete coil wires. Since this linear component is very small for all but the dipole field (since that is the intended field of the magnet), we expect the normalized multipole fields to decay as approximately $1/L$. This can be seen on Figure 5 (right panel).

For a magnet with a physical length of 90 cm, the sextupole component has the largest magnitude with about 2 units. When we increase the layer width, we expect the field quality to decrease.

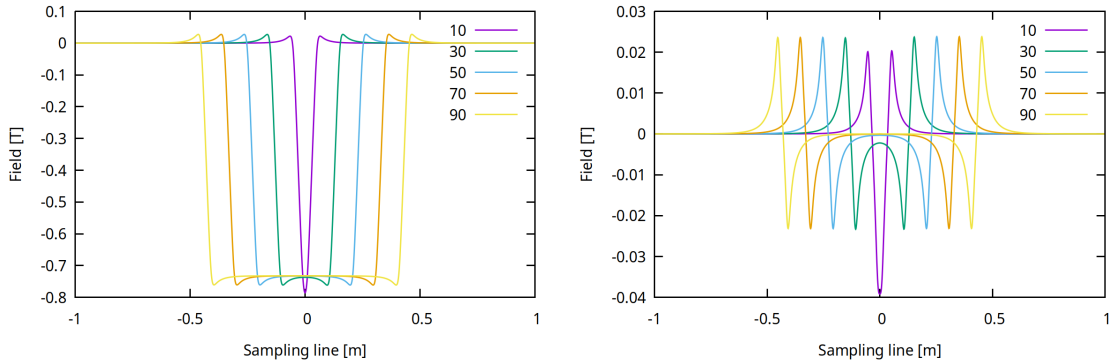

Figure 4: The dipole (left) and quadropole field (right) plotted for various magnet length.

4 Conclusions and outlook

A python code was developed for the construction of the complicated coil end geometry of the opposite field superconducting septum magnet. As input, this algorithm requires the 2D coordinates of the winding cross section, and outputs the full 3D path of the complete winding, using a single superconducting strand without a soldered joint, for one aperture of the twin-aperture magnet. The code has been extended to generate macros for Autodesk Inventor (a 3D CAD design software), which create the parts of the setup natively in the software, facilitating the construction of a prototype of this magnet. An image of the cad model can be

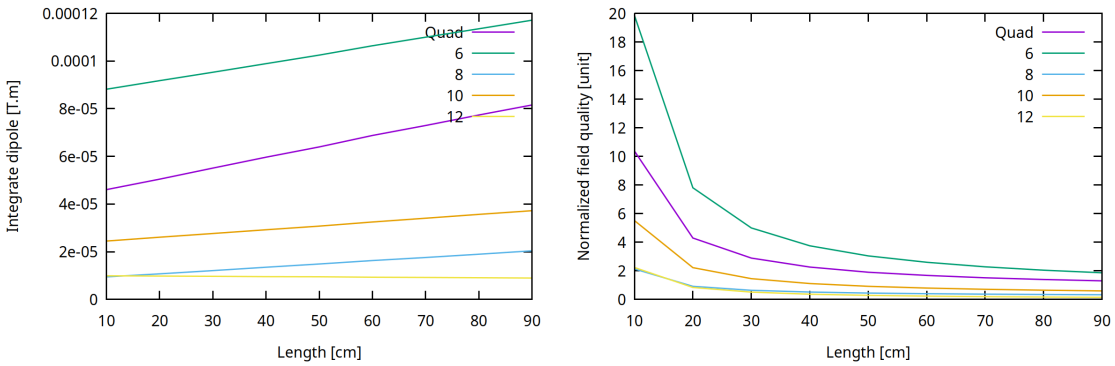

Figure 5: The integrated multipoles (left) and normalized field quality (right)

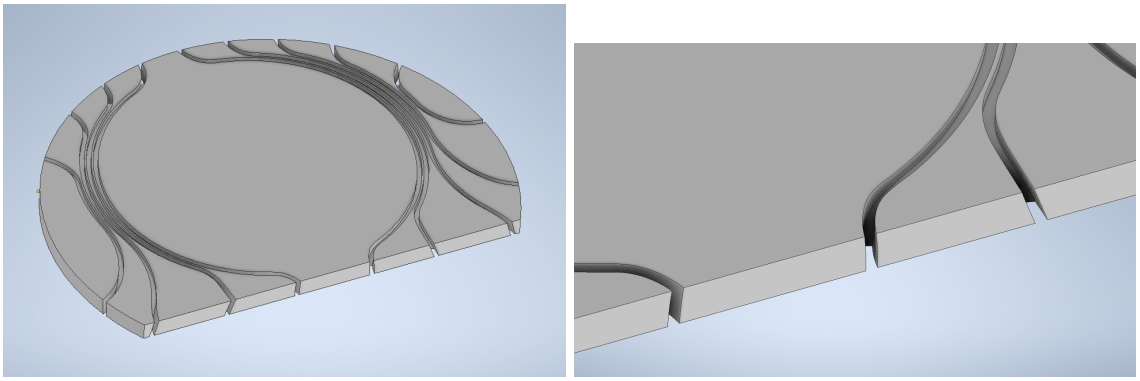

Figure 6: The CAD model for the outermost layer (left) and a closeup showing the complex geometry at then ends, where the wire descends into the material (right)

seen on Fig. 6. The magnetic field of the 3D coil configuration was simulated in RAT and was shown to have a decent field quality for a physical magnet length of the order of 1 m.

Wigner Research Centre for Physics is developing its infrastructure for the winding and vacuum epoxy impregnation of CCT-like magnets, and is preparing for the constuction of the SuShi septum prototype magnet. Building on the experience and the local industrial connections gained during this project, the research group is planning to construct a prototype for the opposite field septum magnet described in this summary.

5 References

References

[1] Dániel Barna and Martin Novák. Two-dimensional conceptual design of a superconducting iron-free opposite field septum magnet. *Nuclear Instruments and Methods in Physics Research Section A: Accelerators, Spectrometers, Detectors and Associated Equipment*, 959:163521, 2020.

[2] Jeroen van Nugteren. Project rat. `https://gitlab.com/Project-Rat/`.